

Scaling law for the transient behavior of type-II neuron models

M. A. D. Roa* and M. Copelli†

*Laboratório de Física Teórica e Computacional, Departamento de Física,
Universidade Federal de Pernambuco, 50670-901 Recife, PE, Brazil*

O. Kinouchi‡

*Faculdade de Filosofia, Ciências e Letras de Ribeirão Preto, Universidade de São Paulo,
Av. dos Bandeirantes 3900, 14040-901, Ribeirão Preto, SP, Brazil*

N. Caticha§

Instituto de Física, Universidade de São Paulo 05508-090, São Paulo, SP, Brasil

We study the transient regime of type II biophysical neuron models and determine the scaling behavior of relaxation times τ near but below the repetitive firing critical current, $\tau = C(I_c - I)^{-\Delta}$. We find generic behavior in such regimes, which should be respected while building simplified models by dimensional reduction. For both the Hodgkin-Huxley and Morris-Lecar models we find that the critical exponent is independent of the numerical integration time step and pertain to the same universality class, with $\Delta = 1/2$. For appropriately chosen parameters, the FitzHugh-Nagumo model presents the same generic transient behavior, but the critical region is significantly smaller. We propose an experiment that may reveal non trivial critical exponents in the squid axon.

PACS numbers: 05.45.-a, 89.75.Fb, 05.90.+m

Computational neuroscience modeling is based on the rich dynamics of biophysical model neurons. Spiking neurons generate tale telling signatures which have served as the basis for frequency dependent neural codes. Although of paramount importance to neural dynamics, average spike frequency does not tell the complete story. In many cases, the key to the information dynamics lies in the transients. In this paper we investigate universal transient properties of conductance-based model neurons by numerical and analytical means. We also propose an experiment that may test our theoretical predictions.

The Hodgkin-Huxley (HH) model is a biophysically motivated system of four coupled non-linear differential equations that describe the dynamics of the membrane potential V of the squid giant axon relative to its resting state (e.g. [1, 2, 3]):

$$\begin{aligned} C \frac{dV}{dt} &= G_{Na} m^3 h (E_{Na} - V) + G_K n^4 (E_K - V) \\ &\quad + G_L (E_L - V) + I(t) \\ \frac{dx_i}{dt} &= \alpha_{x_i}(V)(1 - x_i) - \beta_{x_i}(V)x_i \end{aligned} \quad (1)$$

where x_i stand for the three gate variables $x_i = m, h$ and n describing the activation of ionic channels [3, 4] and $\alpha_{x_i}, \beta_{x_i}$ are voltage dependent transition rates [5].

The HH system plays a fundamental role in the field of neurophysiology and computational neuroscience since it defines the class of conductance based models. As a function of a constant applied current I , the HH model undergoes a subcritical Hopf bifurcation at $I = I_H$, above which the fixed point solution (membrane potential at rest) is no longer stable and trajectories are attracted to a stable limit cycle, leading to repetitive firing (infinite train of action potentials).

This sudden jump to a periodic behavior with nonzero frequency f is analogous to a first order phase transition and is referred to as type II behavior in the neuroscience literature [6]. Like in first order phase transitions, coexistence also appears in type II behavior. Just below the Hopf bifurcation, the stable fixed point coexists with a stable limit cycle, their basins of attraction being separated by an unstable limit cycle [6]. Both limit cycles are born in a saddle-node (or “fold”) bifurcation of cycles at $I = I_c < I_H$. In our analogy with equilibrium phase transitions, I_c would correspond to a spinodal point. If the fixed point at $I = 0$ is perturbed by the application of a constant current near but below I_c , several spikes may appear before the system returns to the new resting state (Fig. 1).

In the original version of the Morris-Lecar (ML) model [7], a system with two coupled non-linear ODEs originally used to describe action potentials in a barnacle motor fiber, the relevant bifurcation at the onset of repetitive firing is a saddle-node one. That means that the spiking frequency varies continuously from I_c as $f \propto (I - I_c)^\beta$, with $\beta = 1/2$, which is similar to a mean field second order phase transition behavior if we think of f as the order parameter. This transition is called type I behavior in the neuroscience literature [6] and does not present the slow transient phenomenon similar to Fig. 1.

*Electronic address: mdr1angel@df.ufpe.br

†Electronic address: mcopelli@df.ufpe.br

‡Electronic address: osame@ffclrp.usp.br

§Electronic address: nestor@if.usp.br

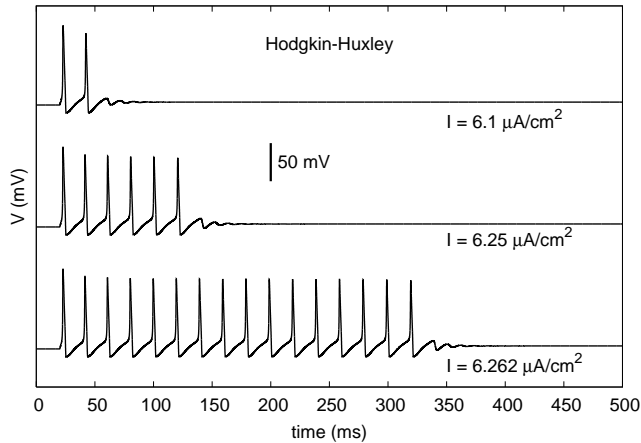


FIG. 1: Examples of transient behavior near I_c for the HH model. The constant step current is applied at $t = 10$ ms. The estimated critical current is $I_c = 6.26422125685 \mu\text{A}/\text{cm}^2$ for an integration time step $dt = 0.01$ ms.

However, the parameters of the Morris-Lecar system can be tuned so that it presents a type II behavior [6, 8]:

$$\begin{aligned} C \frac{dV}{dt} &= 0.5G_{Ca} \left[1 + \tanh\left(\frac{V+1}{15}\right) \right] (E_{Ca} - V) \\ &\quad + G_K w (E_K - V) + G_L (E_L - V) + I(t) \\ \frac{dw}{dt} &= 0.1 \cosh(V/60) [1 + \tanh(V/30) - 2w] . \end{aligned} \quad (2)$$

In this case, large transient times are also observed (Fig. 2).

The FitzHugh-Nagumo (FHN) system

$$\begin{aligned} \frac{dV}{dt} &= V(V-a)(1-V) - W + I \\ \frac{dW}{dt} &= \epsilon(V - \gamma W) , \end{aligned} \quad (3)$$

has been proposed as a low-dimensional toy model that represents the type-II behavior of the HH and other excitable systems. We verified that the transient behavior here reported is not seen with the usual parameters used in the literature [3]. However, we believe that modelling should not be aimed only at reproducing stationary behavior (attractors) but also the transient behaviors that might be lost during the procedure of dimensional reduction. The FHN model can reproduce the HH transient behavior if one chooses parameters near $a = 0.5$, $\gamma = 4.2$ and $\epsilon = 0.01$ (Fig. 3). If other values are chosen we still suggest care should be taken in order to respect the transients.

In this paper we show that the long relaxation times in type-II models are a consequence of the changes in phase space which occur near the birth of the limit cycles. Moreover, this leads to a scaling relation whose

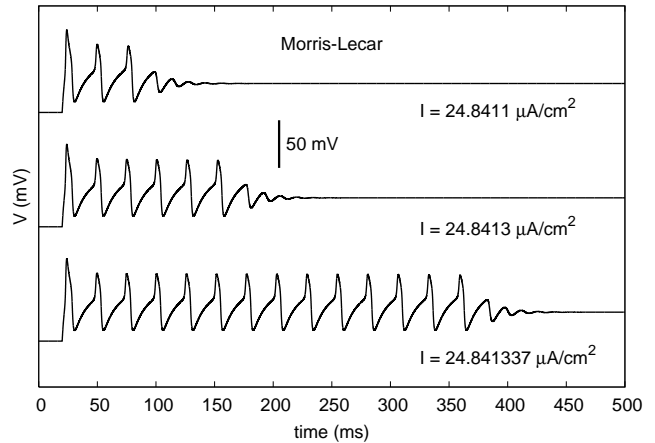


FIG. 2: Examples of transient behavior near I_c for the ML system. The constant step current is applied at $t = 10$ ms. The estimated critical current is $I_c = 24.84134676279 \mu\text{A}/\text{cm}^2$ for an integration time step $dt = 0.01$ ms.

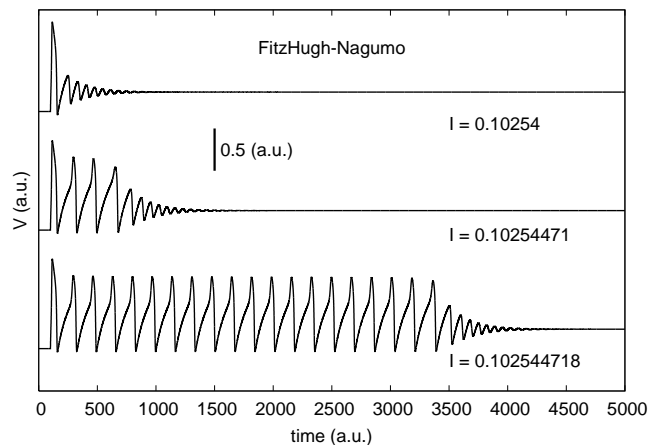


FIG. 3: Examples of transient behavior near I_c for the FHN system. The constant step current is applied at $t = 10$ ms. The estimated critical current is $I_c = 0.1025447183127$ for an integration time step $dt = 0.01$.

exponent can be predicted, in agreement with numerical simulations. The relaxation time τ may be defined as the time until the last spike, or the time until the membrane voltage stays within a small distance from the resting potential (these two times are very similar near I_c). When we plot τ as a function of $I_c - I$ we find a power law divergence of the relaxation time, $\tau \simeq C(I_c - I)^{-\Delta}$, where Δ is similar to a dynamic critical exponent. The Δ exponent characterizes the “critical slowing down” behavior near the bifurcation. We expect that Δ is a universal exponent but we are not aware that this exponent has been measured for neuron models. Here we report the measured exponents for these three type-II biophysical neu-

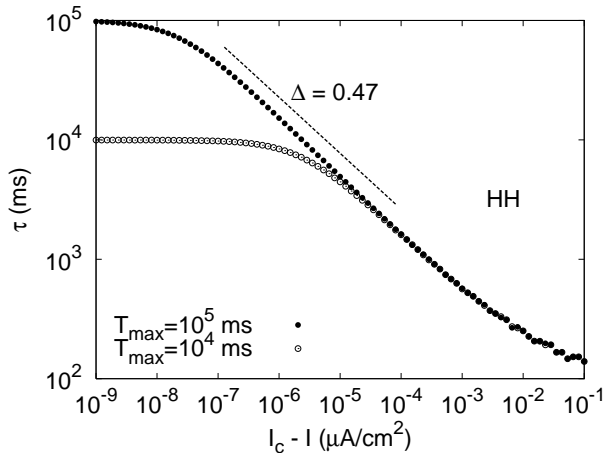


FIG. 4: Relaxation times for the HH model as a function of the distance to critical current for different integration times: $T_{max} = 10^4$ ms (open circles) and $T_{max} = 10^5$ ms (filled circles).

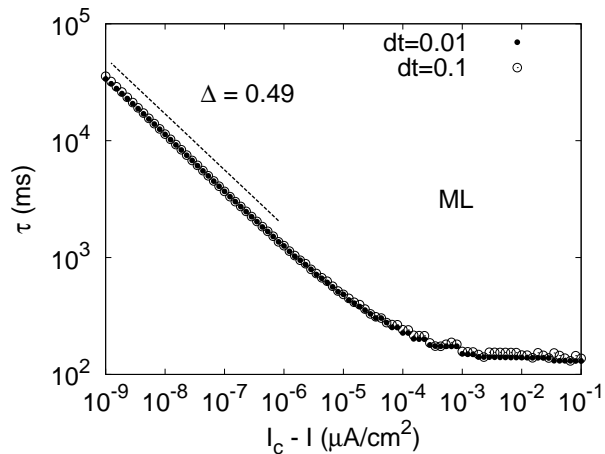


FIG. 5: Relaxation times for the Morris-Lecar model as a function of the distance to critical current for different integration times: $dt = 0.01$ ms (filled circles) and $dt = 0.1$ ms (open circles).

ron models, finding very good agreement between them.

We integrated the equations using a standard fourth-order Runge-Kutta algorithm and determined τ by measuring the time interval from the onset of the current step to a near stop of the flow ($|\dot{\mathbf{x}}| < \delta = 10^{-5}$, where $\dot{\mathbf{x}}$ is the instantaneous velocity vector in phase space). As opposed to the Hopf bifurcation, the fold bifurcation cannot be obtained analytically, so I_c was estimated numerically after integration of the ODEs up to a (long) maximum time T_{max} . The determination of the critical current is sensitive on T_{max} , but in practice this only limits the range of validity of the power law (see Fig. 4). We have employed $T_{max} = 10^5$ ms and $dt = 0.01$ ms, unless otherwise stated. The estimated critical currents

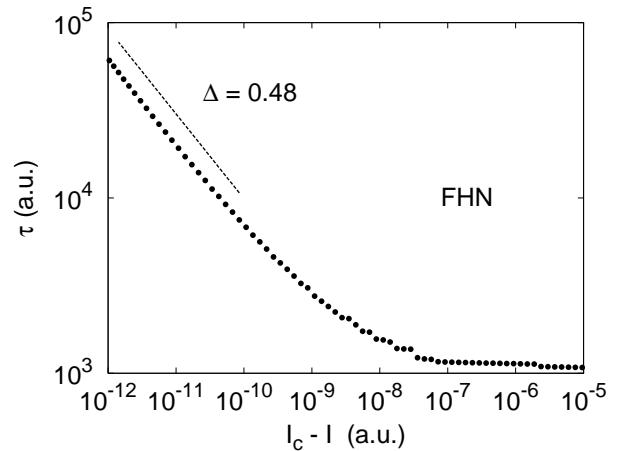


FIG. 6: Relaxation times for the FitzHugh-Nagumo model as a function of the distance to critical current. Note that the power law becomes visible only *very* close to the fold bifurcation ($I_c - I \sim 10^{-9}$).

$I_c(T_{max}, dt)$ quoted in the figure captions are very precisely determined *given* T_{max} and the integration step size dt . While the result is numerically arbitrarily precise for each (T_{max}, dt) , the accuracy of the actual critical current $I_c(T_{max} \rightarrow \infty, dt \rightarrow 0)$ should in no way be thought to be represented by the huge number of decimal figures.

The critical exponent is determined from the plot τ vs $I_c - I$. We found $\Delta = 0.47$ for the HH system (Fig. 4) and $\Delta = 0.49$ for the ML model (Fig. 5), irrespective of the size of the integration step dt . This suggests a universal exponent $\Delta = 1/2$. Obtaining long transients in the FHN model has proved numerically more difficult, since the phenomenon seems to occur only very close to I_c (Fig. 6). Nonetheless, we have obtained the exponent $\Delta = 0.48$.

Figure 7a shows that for $I_c \lesssim I < I_H$ an unstable and a stable limit cycles coexist and surround a stable fixed point. The fixed point for $I = 0$ lies outside both limit cycles (Fig. 7b). Therefore, when the current is abruptly changed to $I \lesssim I_c$, the fixed point is displaced to a region within a “ghost limit cycle”, and the transient is completely dominated by the time it takes for the system to overcome it. The “ghost” is a natural consequence of the system being immediately below a saddle-node bifurcation of cycles, and can be characterized by the vanishingly small flow component normal to the half-stable limit cycle that is born at $I = I_c$. It effectively works as a one-dimensional extended bottleneck through which the system must pass before reaching the fixed point. If one considers an analogous system in polar coordinates [9] $\dot{\theta} = f(r, \theta)$, $\dot{r} = \mu r + r^3 - r^5$, where $f(r, \theta) > 0, \forall r > 0$, it is clear that for $\mu \lesssim \mu_c = -1/4$ the time for the system to overcome the “ghost” at $r = 1/2$ scales as $\tau \sim (\mu_c - \mu)^{-1/2}$ (the Hopf bifurcation occurring only at $\mu_H = 0$). Solutions for the transient behav-

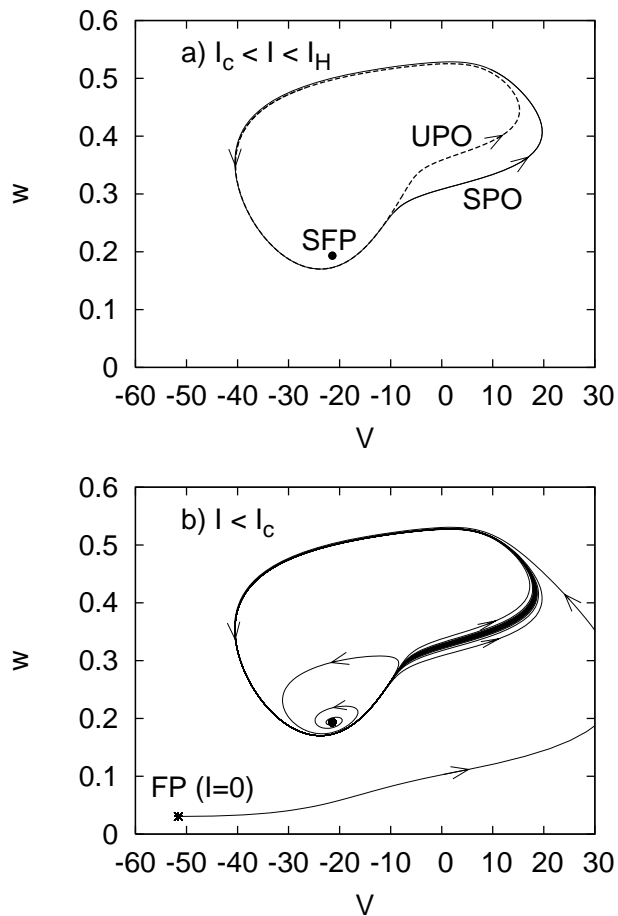


FIG. 7: Phase portraits of the ML model for I slightly above (a) and below (b) I_c . The long transient is dominated by the time it takes to pass through the region where the limit cycles are about to emerge.

ior have been obtained by Tonnelier [10] for McKean’s piecewise linear version of the FHN model [11]. However, the scaling behavior has not been observed because

the model has been studied in the absence of an external current.

It is interesting to point out that this bottleneck effect is analogous to what occurs for type-I neurons *above* the saddle-node bifurcation that leads to repetitive firing. In that case, however, the “ghost” results from the annihilation of fixed points (not limit cycles) and the *period* T of the limit cycles diverges as $(I - I_c)^{-1/2}$. This provides a complementary scenario connecting both classes of neurons: the transient of type-II models below I_c diverges with the same exponent as the period of type-I models above I_c , that is, $\Delta = \beta$.

We were unable to find a description of this scaling law behavior for transients in neuron models or the associated dynamic critical exponent in the literature, so perhaps this is the first report about this phenomenon. Some kind of critical slowing down for subthreshold oscillations have been reported experimentally in the squid axon [12], but these authors examined the vicinity of a parametric subcritical Hopf bifurcation, not a saddle-node bifurcation of cycles induced by external currents. We propose that a similar experiment with high precision injected currents near the critical current I_c could be used to check the power law phenomenology found in the computational model.

We emphasize that both in standard experiments and in our single compartment model, space clamp is used. It might happen though, as in spin systems, that for the extended real system without voltage clamp, or for a compartmental model with large number of compartments, the exponents may differ from the values here reported, changing the universality class to one not described by a “mean field” approach. Interestingly, this would mean that collective properties within a non-trivial universality class could be observed at the level of a single axon.

Acknowledgments: Research supported by FACEPE, CNPq and special program PRONEX. This work has been initiated during the LASCON - Latin American School on Computational Neuroscience and MADR thanks the organizers for financial support.

-
- [1] D. Johnston and S. M.-S. Wu, *Foundations of Cellular Neurophysiology* (MIT Press, Cambridge, 1995).
 [2] J. M. Bower and D. Beeman, *The Book of GENESIS: Exploring Realistic Neural Models with the General NEural Simulation System* (Springer-Verlag, 1995).
 [3] C. Koch, *Biophysics of Computation* (Oxford University Press, New York, 1999).
 [4] $C = 1 \mu\text{F}/\text{cm}^2$ is the specific membrane capacitance, $G_{Na} = 120 \text{ mS}/\text{cm}^2$, $G_K = 36 \text{ mS}/\text{cm}^2$ and $G_L = 0.3 \text{ mS}/\text{cm}^2$ are ionic conductances per unit area, $E_{Na} = 115 \text{ mV}$, $E_K = -12 \text{ mV}$, $E_L = 10.6 \text{ mV}$ are reversal potentials.
 [5] $\alpha_m(V) = \frac{2.5-0.1V}{e^{(2.5-0.1V)}-1}$; $\beta_m(V) = 4e^{-V/18}$; $\alpha_h(V) = 0.07e^{-V/20}$; $\beta_h(V) = \frac{1}{e^{(\beta-0.1V)}+1}$; $\alpha_n(V) =$

- $\frac{0.1-0.01V}{e^{(1-V)}-1}$; $\beta_n(V) = 0.125e^{-V/20}$.
 [6] J. Rinzel and B. Ermentrout, in *Methods in Neuronal Modeling: From Ions to Networks*, edited by C. Koch and I. Segev (MIT Press, 1998), pp. 251–292, 2nd ed.
 [7] C. Morris and H. Lecar, *Biophys. J.* **35**, 193 (1981).
 [8] $G_{Ca} = 1.1 \text{ mS}/\text{cm}^2$, $G_K = 2.0 \text{ mS}/\text{cm}^2$, $G_L = 0.5 \text{ mS}/\text{cm}^2$, $E_{Ca} = 100 \text{ mV}$, $E_K = -70 \text{ mV}$ and $E_L = -50 \text{ mV}$.
 [9] S. H. Strogatz, *Nonlinear Dynamics and Chaos: with Applications to Physics, Biology, Chemistry and Engineering* (Addison-Wesley, Reading, MA, 1997).
 [10] A. Tonnelier, *SIAM J. Appl. Math.* **63**, 459 (2002).
 [11] M. P. McKean, *Adv. Math.* **4**, 209 (1970).
 [12] G. Matsumoto and T. Kunisawa, *J. Phys. Soc. Japan* **44**, 1047 (1978).